Korean J. Chem. Eng., 39(3), 504-514 (2022)
DOI: 10.1007/s11814-021-0864-7

pISSN: 0256-1115
eISSN: 1975-7220

Incipient fault diagnosis for centrifugal chillers using kernel entropy component analysis and voting based extreme learning machine

Yudong Xia*, Qiang Ding*,†, Aipeng Jiang*, Nijie Jing*,, Wenjie Zhou*, and Jian Wang***

*School of Automation (School of Artificial Intelligence), Hangzhou Dianzi University, Hangzhou, China
**Institute of Refrigeration and Cryogenics, Zhejiang University, Hangzhou, China
(*Received 13 April 2021 • Revised 25 May 2021 • Accepted 2 June 2021*)

Abstract−Incipient fault detection and diagnosis for centrifugal chillers is significant for maintaining safe and effective system operation. Due to the advantages of simple learning algorithm and high generalization capability, the extreme learning machine (ELM) can identify faults quickly and precisely in comparison to conventional classification methods such as back propagation neural network (BPNN). This paper reports an effective diagnosis method for incipient chiller faults with the integration of kernel entropy component analysis (KECA) and voting based ELM (VELM). KECA was first performed to reduce the dimensionality of the original input data so as to minimize the model complexity and computational cost. Instead of using a single ELM, multiple independent ELMs were adopted in VELM, and then the class label could be predicted based on the majority voting method. Using the experimental data of seven typical faults together with a normal operation, the proposed KECA-VELM fault diagnostic model was trained and further validated. The results show that a better fault diagnosis performance can be achieved using the KECA-VELM classifier compared with the conventional BPNN, ELM and VELM based classifiers. The overall average fault diagnosis accuracy for the faults at the least severity level was reported over 95% based on the proposed method.

Keywords: Operational Safety, Fault Diagnosis, Water Chillers, Extreme Learning Machine, Kernel Entropy Component Analysis

INTRODUCTION

Centrifugal chillers are one of the most widely used heating, ventilation and air conditioning (HVAC) systems in buildings. In comparison to direct expansion (DX) type A/C systems, water chillers are more advantageous in large-scale buildings, in terms of a wider operational range, a higher system efficiency and a better part-load characteristic. At the end of 2017, nearly five million water chillers were in service in China [1]. It was reported that nearly 9.2% of building energy consumption was by space air conditioning (A/C) in 2016 [2]. However, unexpected chiller faults may emerge after a long-time system operation. The presence of chiller faults in routine operation is one of the most significant challenges in building automation systems, negatively affecting the system reliability and energy efficiency. Chiller faults have accounted for about 42% of the service resources and approximately 26% of the repair costs [3]. Therefore, it is of significance to seasonally detect and diagnose the chiller anomalies for the energy saving of buildings.

In view of the knowledge used for formulating diagnostic systems, the fault detection and diagnosis (FDD) methods can be classified into three categories: quantitative model-based, qualitative model-based, and process history based [4,5]. Compared to the first two groups where a priori knowledge of a process is assumed, only historical data are required for the third approach, and thus it has gained a wider application. The process history-based methods include gray-box models and black-box models. The first one use first principles to establish the empirical model where its parameters, such as coefficients in the model, are identified from historical data, such as the state observer based [6] and the Kalman filter based [7] models. With the increasing complexity of building energy systems, data-driven approaches have been regarded as promising for building performance simulation, benchmarking analysis, control optimization, as well as FDD in buildings [8]. Over the decades, data-driven approaches have been extensively adopted for FDD of HVAC systems, including vapor compression refrigeration systems [9], variable refrigerant flow (VRF) systems [10,11], air handling units (AHUs) [12,13] and water chillers [14-16].

The data-driven fault diagnosis for HVAC systems can be regarded as a typical kind of multiclass classification problem, and its representative approaches mainly include artificial neural network (ANN) and support vector machine (SVM). Du et al. [17] proposed a sensor fault diagnosis scheme for variable air volume systems with the application of wavelet analysis and neural network. Wavelet analysis was adopted for original data processing, and the neural network trained to diagnose the source of fault. Later, a dual neural network combining basic neural network with auxiliary neural network was developed by Du et al. [18] for recognizing the anomalies in an AHU. Using the dual neural networks, the detection performance was improved as expressed in terms of a lower false alarm and shorter detection time. To optimize the feature extraction, association rule mining algorithm was applied to select the appropriate features in a VRF system, and a so-called optimized back propaga-

†To whom correspondence should be addressed.
E-mail: dingqiang@hdu.edu.cn

tion (BP) neural network method was proposed by Guo et al. [11] for formulating the fault diagnostic system. As a multilayer perceptron, when using the conventional ANN for multiclass classification, unexpected problems, such as local minima, slow learning rate, and risk of over-fitting, may be encountered, leading to poor fault diagnosis. SVM is another popular classifier widely adopted for fault diagnosis. Unlike the conventional ANN, SVM first maps the training data into a high-dimensional space via introducing a nonlinear feature function and then tries to maximize the separating margin of two different classes in the feature space and at the same tine minimizing training errors using conventional optimization methods [19]. Therefore, SVM has a relatively high generalization capability. Liang and Du [20] developed a multi-layer SVM classifier to diagnose the faults in a single zone HVAC system. Han et al. [21] proposed a one-against-one multi-class SVM based chiller fault diagnosis method with its kernel parameters being tuned by genetic algorithm optimizer. Results showed that significant improvement in fault diagnosis performance was achieved for the faults of refrigerant leak and refrigerant overcharge. Yan et al. [22] studied a hybrid FDD method for water chillers which incorporated an auto-regressive model with exogenous variables and SVM. The FDD performance was compared to that in case of using the multilayer perceptron neural network classifier, demonstrating the superiority of the proposed method in terms of a higher prediction accuracy and lower false alarm rates. As a matter of fact, the training of SVMs is a quadratic programming, and thus its computational complexity is usually intensive. Moreover, when using SVM for multiclass classification, at least two hyperparameters are required to be specified and optimized, which is not an easy task in practical applications. Furthermore, another primary challenge in chiller FDD is the difficulty in timely identifying the faults at their incipient stages. A lower fault severity level will have less impact on the system operation, and thus the incipient faults tend to be more difficult to recognize. For example, the diagnosis accuracy for the incipient faults of refrigerant over charging and lubricant over charging was only 48% and 54.3%, respectively, in a recently reported study [23]. Therefore, more effects should be done to the enhanced fault diagnosis performance of the incipient chiller faults.

Recently, extreme learning machine (ELM) algorithm for single hidden layer feedforward neural networks (SLFNs) was proposed by Huang et al. [24] and has been merged as an efficient learning algorithm for SLFNs. ELM employs classification by mapping the input data to a high dimensional space and then transforms the classification task to a multi-output function regression problem. In ELM, the input weights and hidden biases are assigned randomly, the output weights are calculated by Moore-Penrose (MP) generalized inverse, and thus the hidden layer needs not be tuned. Therefore, ELM achieves higher scalability and less computation complexity than the aforementioned algorithms, BP neural network and SVM [25]. It has been successfully adopted in an extensive variety of applications, including face recognition [26,27], data prediction [28,29] and FDD [30,31]. Currently, for overcoming the problems of misclassification for the data near the nonlinear classification boundary, Cao et al. [32] proposed a voting based ELM (VELM) algorithm. Instead of using a single ELM training, multiple independent ELM based classifiers are trained simultaneously, then the final decision is made by the majority voting method. Therefore, VELM outperforms the conventional ELM with an enhanced classification performance. However, no studies on chiller fault diagnosis using ELM can be identified in open literature. Therefore, one of objectives in the current study is to establish a VELM algorithm based diagnostic systems for incipient faults in water chillers.

On the other hand, before performing the classification, data decomposition is generally required for reducing the modelling complexity and computational cost. In view of the FDD methods used for HVAC systems, principal component analysis (PCA) is one of the most widely adopted algorithms [14-16,33-35]. PCA is a linear data decomposition method preserving maximally the second-order statistics of the original data, and thus it may not be suitable for tackling the problems of nonlinear data transformation of water chillers. Recently, Rényi entropy has been introduced in the traditional PCA to compute the information carried by the original data, and a so-called kernel entropy component analysis (KECA) method was proposed by Jenssen [36]. Unlike PCA, KECA performs data decomposition in a high-dimensional kernel space which is nonlinearly related to the input data space, and tries to preserve the maximum Rényi entropy of the original data. Recent studies have indicated that KECA is a promising tool for nonlinear data transformation [37,38]. For example, Xia et al. [37] proposed an effective fault detection method using KECA algorithm for water chillers. Results showed that a higher fault detection rate could be acquired in comparison to the traditional PCA, demonstrating the advantageous of KECA for dimensionality reduction.

Consequently, this paper reports the development of an effective fault diagnosis method for water chillers with the integration of KECA and VELM. The paper is organized as follows. First, the KECA and VELM algorithms are briefly reviewed in Section 2. In section 3, the structure of the proposed KECA aided VELM based fault diagnostic system for water chillers is detailed. Section 4 presents the validation results based on the experimental data from ASHRAE RP-1043. Finally, the main contributions of the current study are concluded in Section 5.

METHODS AND PRINCIPLES

1. Kernel Entropy Component Analysis

Given a data set, D: $\mathbf{x}_1$, $\mathbf{x}_2$, …, $\mathbf{x}_n$, its Rényi quadratic entropy [39] can be estimated as

$$H_2(p) = -\log\left[\int_{-\infty}^{\infty} p^2(\mathbf{x})d\mathbf{x}\right] \quad (1)$$

where, $p(\mathbf{x})$ is the probability density function generating this data set. Letting $V(p)=\int_{-\infty}^{\infty} p^2(\mathbf{x})d\mathbf{x}$ and introducing a Parzen window density estimator [40] yields

$$\hat{p}(x) = \frac{1}{n}\sum_{x_t \in D} K(\mathbf{x}, \mathbf{x}_t|\sigma) \quad (2)$$

Here, $K(\mathbf{x}, \mathbf{x}_t|\sigma)$ is the Parzen window, conventionally known as kernel centered at $\mathbf{x}_t$. σ is the width parameter of the kernel. Applying the Gaussian or radial basis function, namely, $k(\mathbf{x}_t, \mathbf{x}_{t'})=\exp(-||\mathbf{x}_t-\mathbf{x}_{t'}||^2/$

$2\sigma^2$), yields [41],

$$\hat{V}(p)=\frac{1}{n}\sum_{i=1}^{n}\frac{1}{n}\sum_{j=1}^{n}K(\mathbf{x}_t, \mathbf{x}_{t'}|\sqrt{2\sigma})=\frac{1}{n^2}\mathbf{I}^T\mathbf{K}\mathbf{I} \tag{3}$$

where $\mathbf{K}$ is the kernel matrix and equals $K(\mathbf{x}_t, \mathbf{x}_{t'}|\sqrt{2\sigma})$, $\mathbf{I}$ the (n×1) vector of ones. The Renyi entropy estimate, $V(\hat{p})$, hence can be estimated using the available sample fully residing in the elements of the corresponding kernel matrix, $\mathbf{K}$, which can be eigen-decomposed as $\mathbf{K}=\mathbf{E}\mathbf{D}\mathbf{E}^T=(\mathbf{E}\mathbf{D}^{0.5})(\mathbf{D}^{0.5}\mathbf{E}^T)$. $\mathbf{D}$ is a diagonal matrix storing the eigenvalues $\lambda_1, \ldots, \lambda_n$ and $\mathbf{E}$ is an eigenvector matrix consisting of the corresponding eigenvectors $\mathbf{e}_1, \ldots, \mathbf{e}_n$. Thus, the Rényi entropy estimate can be evaluated as

$$\hat{V}(p)=\frac{1}{n^2}\sum_{i=1}^{N}(\sqrt{\lambda_i}\mathbf{e}_i^T\mathbf{I})^2=\frac{1}{n^2}\sum_{i=1}^{N}\psi_i \tag{4}$$

$$\psi_i=(\sqrt{\lambda_i}\mathbf{e}_i^T\mathbf{I})^2 \tag{5}$$

ψ_i is the Rényi entropy for each element in Eq. (4). As seen in Eq. (5), both the eigenvalues and the corresponding eigenvectors contribute to the Rényi entropy estimate. Finally, KECA selects those eigenvalues and corresponding eigenvectors according to the first s largest contribution to the entropy estimate, and thus it can be regarded as an *s*-dimensional data decomposition: $\mathbf{P}=\mathbf{K}\times\mathbf{E}_s^T$.

2. Voting Based Extreme Learning Machine

2-1. Extreme Learning Machine

The ELM for an SLFN is schematically shown in Fig. 1. As an SLFN, the structure of ELM is similar to that of a conventional neural network consisting of an input layer, a hidden layer and an output layer. In ELM, the output weights, $\boldsymbol{\beta}$, are calculated by Moore-penrose (MP) generalized inverse, and thus the hidden layer needs not be tuned. Given n arbitrary training samples $\{(\mathbf{x}_i, \mathbf{t}_i)\}_{i=1}^n$, where $\mathbf{x}_i\in R^d$ and $\mathbf{t}_i\in R^m$, the output of a SLFN with L hidden nodes can be mathematically expressed as

$$\mathbf{o}_i=f_i(\mathbf{x}_i)=\sum_{j=1}^{L}\boldsymbol{\beta}_j h(\mathbf{x}_i)=h(\mathbf{x}_i)\boldsymbol{\beta}, \; i=1, 2, \cdots, n \tag{6}$$

$$\mathbf{O}=\mathbf{H}\boldsymbol{\beta} \tag{7}$$

where, $\boldsymbol{\beta}=[\boldsymbol{\beta}_1, \boldsymbol{\beta}_2, \ldots, \boldsymbol{\beta}_L]$ is the weight vector connecting the hidden layer nodes and the output layer nodes. $h(\cdot)$ is the activation function, or the feature mapping function. In the current study,

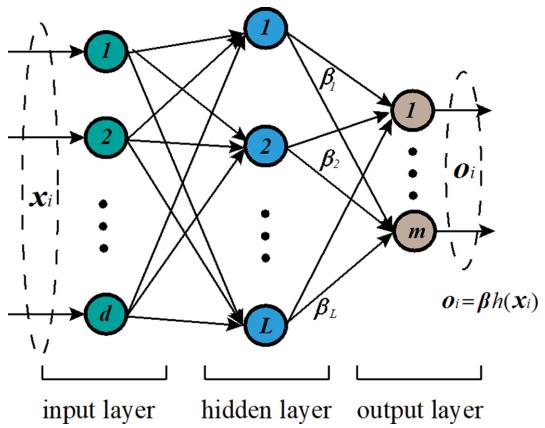

Fig. 1. Structure of ELM based SLFN.

the sigmoid function was selected as the activation function. The hidden layer output matrix, $\mathbf{H}$, can be evaluated as

$$\mathbf{H}=\begin{bmatrix} h(\mathbf{x}_1) \\ \vdots \\ h(\mathbf{x}_n) \end{bmatrix}=\begin{bmatrix} h(\mathbf{w}_1^T\mathbf{x}_1+b_1) & \cdots & h(\mathbf{w}_L^T\mathbf{x}_1+b_L) \\ \cdots & \ddots & \cdots \\ h(\mathbf{w}_1^T\mathbf{x}_n+b_1) & \cdots & h(\mathbf{w}_L^T\mathbf{x}_n+b_L) \end{bmatrix} \tag{8}$$

where $\mathbf{w}_i$ is the weight vector connecting the ith hidden node and the input nodes, b_i is the threshold of the *i*th hidden node. The ith column of the hidden layer output matrix, $\mathbf{H}$, is the *i*th hidden node output corresponding to the inputs $\mathbf{x}_1, \mathbf{x}_2, \ldots, \mathbf{x}_n$, while its *j*th row is the hidden layer feature mapping corresponding to the *j*th input $\mathbf{x}_j$.

Consequently, ELM tries to minimize the training error, namely, $\|\mathbf{O}-\mathbf{T}\|$, and the norm of the output weights, which can be expressed as

$$\text{Minimize: } \|\mathbf{H}\boldsymbol{\beta}-\mathbf{T}\|^2 \text{ and } \|\boldsymbol{\beta}\| \tag{9}$$

where $\mathbf{T}=(\mathbf{t}_1, \mathbf{t}_2, \ldots, \mathbf{t}_n)$ is the target output matrix. In ELM algorithm, its learning parameters, weight $\mathbf{w}_i$ and bias b_i, are randomly assigned initially, and thus the system represented by Eq. (6) becomes a linear one. Consequently, the output weight vector can be computed by finding the least squares solution of Eq. (6):

$$\boldsymbol{\beta}^*=\mathbf{H}^\dagger\mathbf{T} \tag{10}$$

where $\mathbf{H}^\dagger$ is the Moore-Penrose generalized inverse [42] of the hidden layer output matrix $\mathbf{H}$. Finally, given a testing sample, $\mathbf{x}_{test}$, its classification result can be obtained as

$$\mathbf{O}_{test}=\mathbf{H}\boldsymbol{\beta}^* \tag{11}$$

$$\text{label}(\mathbf{x}_{test})=\arg\max f_i(\mathbf{x}_{test}), \; i=1, 2, \cdots, m \tag{12}$$

2-2. Voting Based Extreme Learning Machine

In the conventional ELM algorithm, due to the stochastic learning parameters generated, the samples near the nonlinear separation boundaries may be misclassified, leading to a limited prediction performance. Therefore, in voting based extreme learning machine (VELM), instead of using a single ELM, multiple independent ELM based classifiers are adopted, and the classification results are then obtained through majority voting [32]. Consequently, the classification performance can be further improved.

For easy implementation, the number of hidden nodes and the activation function adopted for all the individual ELMs in VELM are the same. Same training samples are used for training all these individual ELMs, while their learning parameters are initialized independently. Consequently, by majority voting on the classification results predicted by these independent ELMs, the final class label can be obtained.

As shown in Fig. 2, given an s testing sample, $\mathbf{x}_{test}$, there are K independent networks trained by ELM algorithm in VELM. Based on these K independent ELMs, their prediction results can be obtained and then stored to a corresponding vector, $S_{K,\mathbf{x}_{test}}\in R^m$. If the class label predicted by the *k*th ELM is i, the value of the corresponding entry i in the vector $S_{K,\mathbf{x}_{test}}$ is increased by one, which can be expressed as

$$S_{K,\mathbf{x}_{test}}(i)=S_{K,\mathbf{x}_{test}}(i)+1 \tag{13}$$

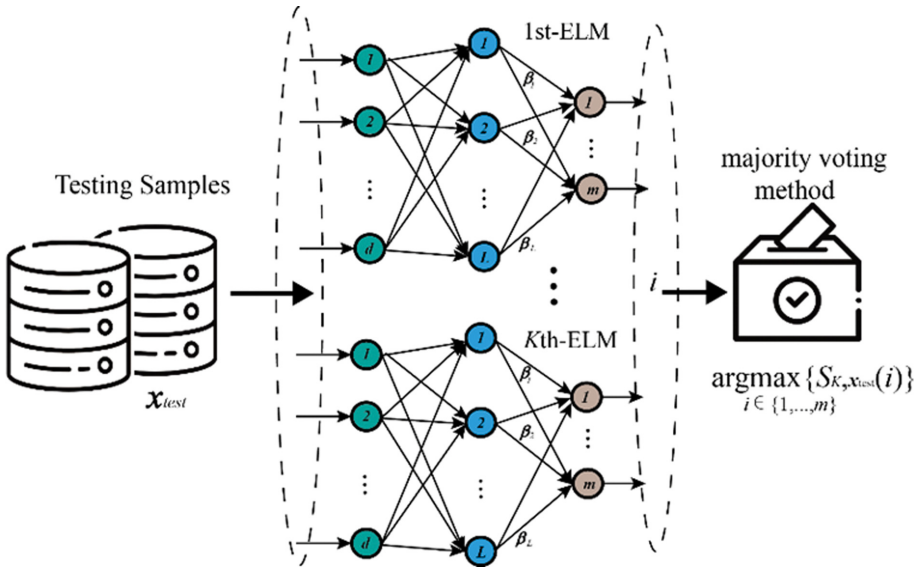

Fig. 2. Structure of VELM for multi-classification.

Consequently, the final class label for the testing sample, $\mathbf{x}_t$, can be determined through employing the majority voting method

$$\text{label}(\mathbf{x}_{test}) = \text{org} \max_{i \in \{1, \ldots, m\}} \{S_{K, \mathbf{x}_{test}}(i)\} \quad (14)$$

STRUCTURE OF THE PROPOSED FAULT DIAGNOSTIC SYSTEM

Through combining the KECA with VELM, the fault diagnos-

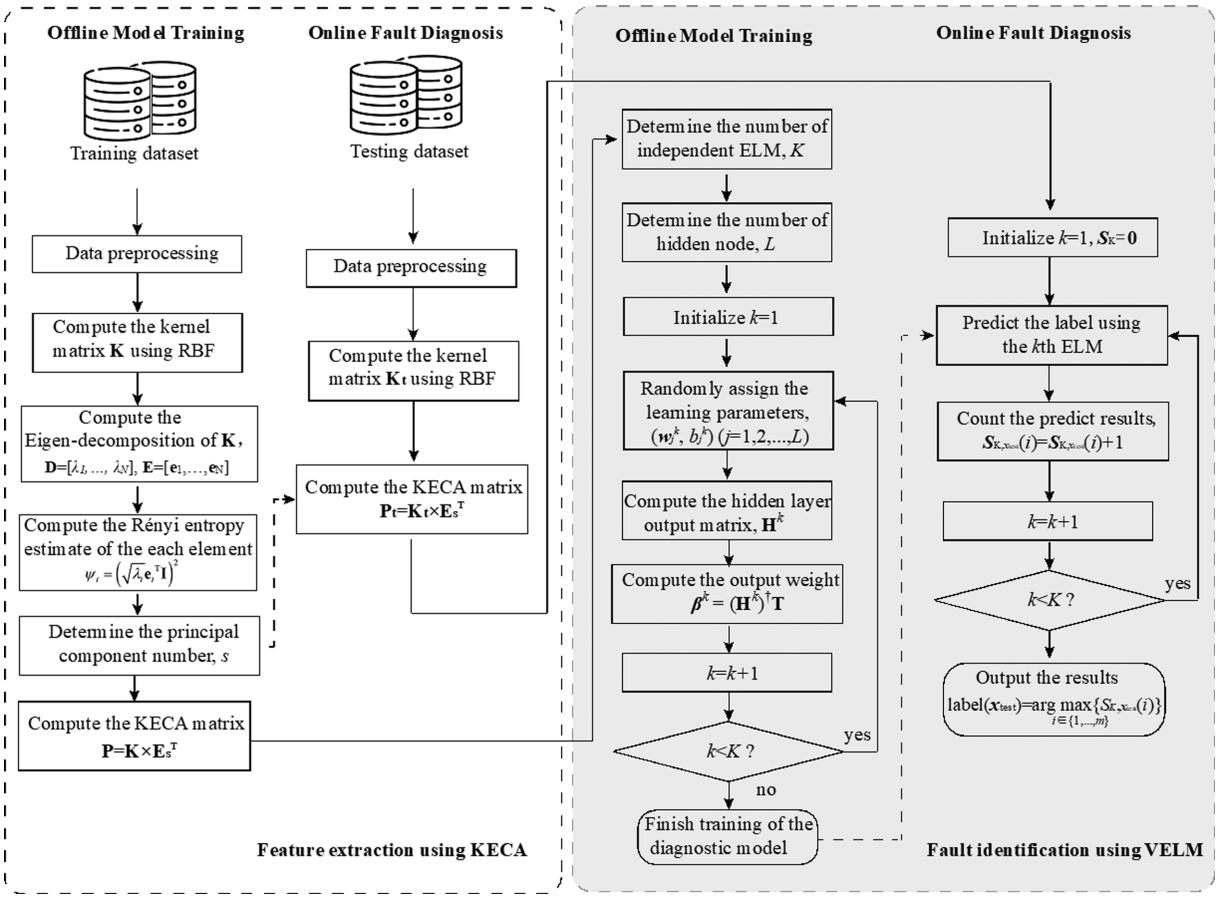

Fig. 3. Structure of the proposed fault diagnostic system for water chillers.

tic system for water chillers can be established. As shown in Fig. 3, the proposed fault diagnostic system includes two parts: feature extraction and fault identification. Feature extraction was performed by KECA, and fault diagnosis was then realized by VELM. In both parts, there are two processes for the development of the fault diagnostic system: the offline model training process and the on-line fault diagnosis process.

1. Offline Model Training

The offline model training process includes two procedures, one for feature extraction and the other for fault diagnostic model training. In the feature extraction part, the input training dataset, $\mathbf{X}_{train}$, including the normal operating samples and the abnormal ones is first filtered and normalized by a data pre-processor. Then, the normalized dataset is nonlinearly mapped onto a high-dimensional kernel feature space using RBK kernel, and the kernel matrix, $\mathbf{K}$, is obtained. Third, the kernel matrix, $\mathbf{K}$, is eigen-decomposed in the kernel feature space by $\mathbf{K}=\mathbf{E}\mathbf{D}\mathbf{E}^T$. This is followed by computing the Renyi entropy estimate using Eq. (5). Fourth, through sorting the Rényi entropy of the dataset in the kernel space, the optimal principal component (PC) number, s, is determined. Finally, the data decomposition of the original input dataset can be achieved by $\mathbf{P}=\mathbf{K}\mathbf{E}_s^T$, and the high-dimensional training dataset, $\mathbf{X}_{train}$, is transformed to the low-dimensional training dataset, $\mathbf{x}_{train}$.

When training the fault diagnostic model using VELM, the numbers of independent ELM and hidden node in each ELM, K and L, are required to be determined first. For kth-ELM, the learning parameters of L-hidden nodes are then randomly assigned by ($\mathbf{w}_j^k$, b_j^k) independently. Third, based on the transformed training dataset, $\mathbf{x}_{train}$, and its corresponding target output dataset, $\mathbf{T}$, the hidden layer output matrix, $\mathbf{H}^k$, is obtained according to Eq (8). This is followed by computing the output weight vector, $\boldsymbol{\beta}^k=(\mathbf{H}^k)^{\dagger}\mathbf{T}$. This training process is not stopped until the output weight vectors for all the individual ELMs are retained, or the training number, k, reaches the pre-defined number of ELM, K. Finally, the fault diagnostic model is established, and the obtained output weight vectors for all the individual ELMs are retained for fault identification.

2. Online Fault Diagnosis

In the online fault detection module, the dimensionality of the testing dataset is initially reduced and then input to the established fault diagnostic model for further fault identification. As shown in Fig. 3, the testing dataset is first filtered and normalized using the previously built data pre-processor. Then it is nonlinearly mapped onto a high-dimensional kernel feature space using the same RBK kernel function, and the kernel matrix for the testing dataset, $\mathbf{K}_t$, is acquired. Third, the dataset in the kernel feature space is projected onto the dominant subspace constructed by the s principal axes, and thus the testing dataset is transformed to a low-dimensional space by $\mathbf{P}_t=\mathbf{K}_t\times\mathbf{E}_s$. Fourth, using the obtained output weight vector, $\boldsymbol{\beta}^k$, the fault label can be predicted based on the k-th ELM by $\mathbf{T}_{test}^k=\mathbf{H}^k\boldsymbol{\beta}^k$. Finally, different types of fault are able to be recognized through majority voting the predicted results of all the individual ELMs as indicated by Eq. (14).

VALIDATION OF THE PROPOSED KECA-VELM FAULT DIAGNOSIS METHOD FOR CHILLERS

1. Experimental System Descriptions

To validate the proposed fault diagnosis method, the real-time

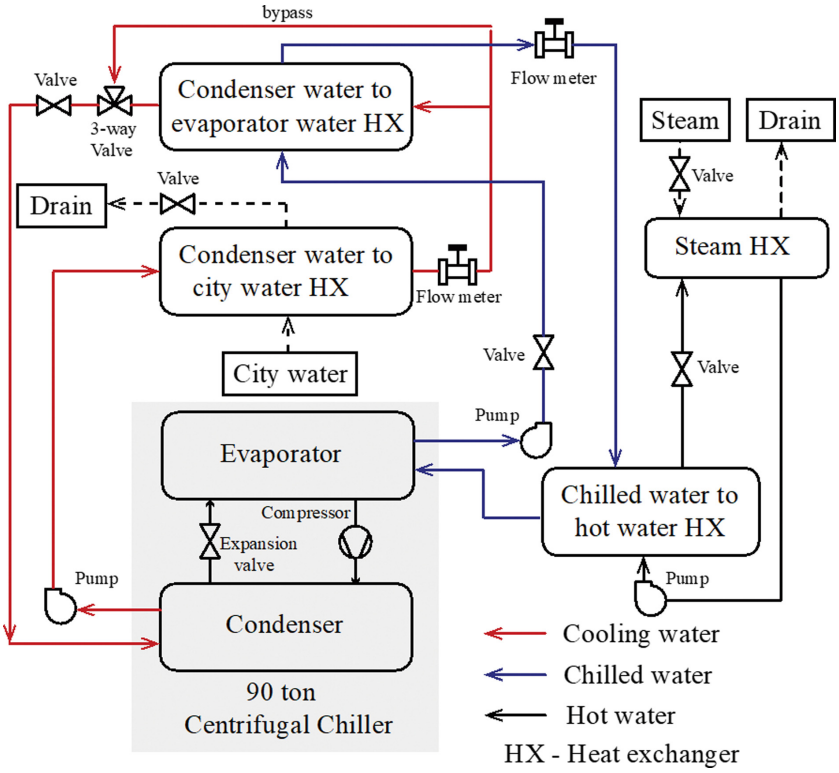

Fig. 4. Schematic diagram of the experimental centrifugal chiller reported in ASHRAE RP1043.

Table 1. Fault types and their corresponding generation methods

Fault code	Fault type	Generation method
0	Normal	Normal operation
1	ReduCF	Reducing water flow rate entering the condenser
2	ReduEF	Reducing water flow rate entering the evaporator
3	ConFoul	Plugging tubes of the condenser
4	NonCon	Adding nitrogen volume
5	RefLeak	Discharging refrigerant weight
6	RefOver	Overcharging refrigerant weight
7	ExcsOil	Increasing lubricant in charge

operating data of a water-cooled chiller reported in the ASHRAE Research Project 1043 (RP-1043) [3] were utilized. The experimental facility is schematically shown in Fig. 4. The 90-ton centrifugal water chiller was equipped with a shell-and-tube evaporator and a shell-and-tube condenser. There were five flow paths in the experimental system: chilled water circuit, cooling water circuit, hot water circuit, the city water supply and the steam water supply. Detailed descriptions of the experimental facility can be found in the report ASHRAE RP 1043 [3].

The experimental system was fully instrumented with highly-precise sensors. 48 operating parameters were directly measured and then used for evaluating the other 16 operating parameters. Therefore, there were 64 input features in the proposed fault diagnostic system. To generate the operating samples with anomalies, different types of faults were manually imposed in the water chiller. The fault types and their corresponding generation methods are shown in Table 1.

Note that for the seven typical faults, each contains four different severity levels, designated by SL1-SL4, corresponding to the least severe fault to the most severe one. As a matter of fact, in chiller routine operation, if a certain kind of fault occurs, its severity level gradually grows with time. Timely identifying the incipient fault is beneficial for reducing equipment downtime, energy waste, and maintenance cost. Hence, incipient fault identification is of vital significance to prevent serious performance deterioration and ensure an optimal system operation. A lower fault severity level will have a less impact on the system operation, and thus the incipient faults tend to be more difficult to recognize in comparison to the serious ones [22,23]. Therefore, in the current research, the seven typical faults at their least severity level together with the normal operation, totally, eight categories, were considered to examine the proposed KECA-VELM fault diagnosis method.

2. Data Pre-processing

Concerning the outliers and transient data between two steady states present in the operating samples, a geometrically weighted variance based filter was adopted to remove these measuring noises. Assuming a set of data $[x_1, x_2, \ldots, x_n]$, its geometrically weighted variance can be evaluated as

$$s_n(\alpha)=\sqrt{\left(\sum_{k=0}^{n}\alpha^{n-k}(x_k-\bar{x}_n(\alpha))^2\right)\Big/\sum_{k=0}^{n}\alpha^{n-k}} \quad (15)$$

where, $\bar{x}_n(\alpha)$ is the geometrically weighted average given by

$$\bar{x}_n(\alpha)=\sum_{k=0}^{n}\alpha^{n-k}x_k\Big/\sum_{k=0}^{n}\alpha^{n-k} \quad (16)$$

$$\alpha=\frac{\tau_{ss}}{(\tau_{ss}+\Delta t)} \quad (17)$$

where τ_{ss} is the effective time window length, Δt the time interval between measurements. Three key operating variables--chilled water supply temperature, inlet water temperatures of the evaporator and condenser--were selected as the indicators of chiller operational state [14]. Consequently, measuring noises were able to be identified if the related data went beyond the slop threshold predefined, and thus could be further removed. The slope threshold and time window length were set at 0.2 °C and 80 s, respectively. Details of this filter can be found in the previous study [37]. Moreover, to ensure all the variables having even contribution, the filtered data were further normalized in the data pre-processor.

3. Dimensionality Reduction

For minimizing the computational complexity, KECA based data decomposition was performed to reduce the data dimensionality and at the same time preserving as much information as possible. As mentioned in Section 3.1, the pre-processed data were projected onto a kernel feature space through nonlinear mapping, and the kernel matrix **K** could be evaluated. Dimensionality reduction hence was then implemented in the high-dimensional kernel feature space via eigen-decomposing of the kernel matrix **K** and

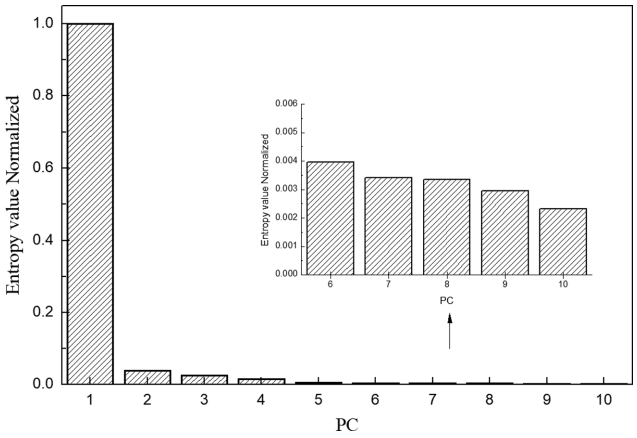

Fig. 5. Normalized Renyi entropies for the top 10 principal components.

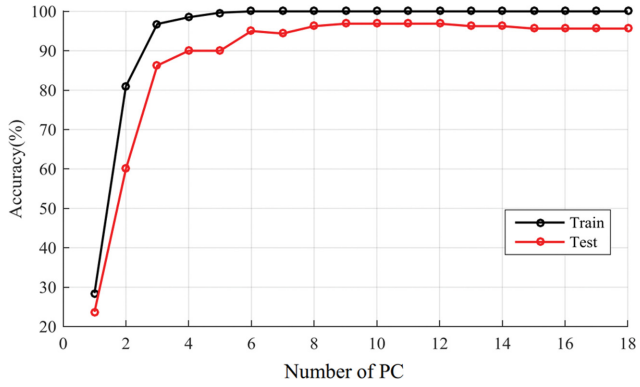

Fig. 6. Variation in fault diagnosis accuracy with the increase of PC number.

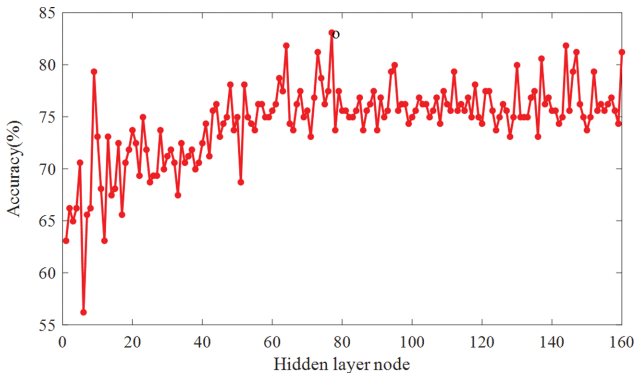

Fig. 7. Fault diagnosis accuracy as increasing the hidden layer nodes.

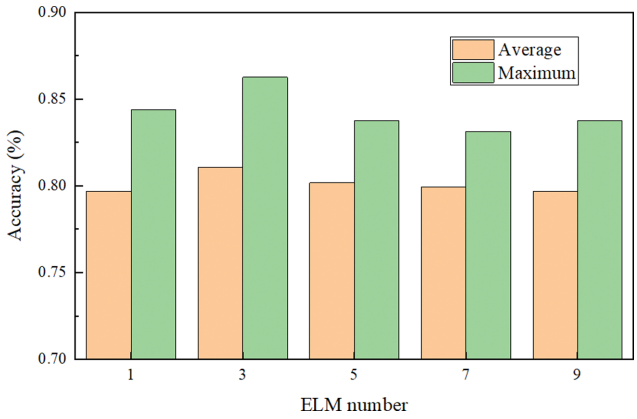

Fig. 8. Fault diagnosis accuracy as increasing the ELM number.

evaluating its corresponding Renyi entropy.

The normalized Renyi entropies for the top ten principal components are shown in Fig. 5. Generally, the optimal number of PC could be obtained through evaluating the cumulative percent variance (CPV) of the first *s* largest Renyi entropies. It was previously shown that the CPV for the first four PCs (PC1-PC4) could reach 96.36% [37], which was enough for data decomposition. In the current study, when training the proposed fault diagnostic model, the number of PC was initially set at 4, and the best diagnosis performance with a reported accuracy of about 90% was achieved. Furthermore, for the enhanced fault diagnosis performance, the fault diagnosis accuracy with the different numbers of PC was also evaluated. As shown in Fig. 6, the fault diagnosis accuracy for both training and testing datasets improved as increasing the PC number. When training the fault diagnostic model, the fault diagnosis accuracy could reach its highest value at 100% based on five PCs. In terms of the model testing results, the highest fault diagnosis accuracy was able to be achieved at 95.6% when the PC number was increased to 9. When further increasing the number of PC, the fault diagnosis accuracy could not be improved. On the other hand, a higher dimensionality of the input gave a more computation complexity. Therefore, for balancing the performance and the model complexity, the optimal PC number, s, was set at 9. Consequently, the dominant subspace was constructed by the principal axes corresponding to the top nine largest Renyi entropies, namely, PC1-PC9, when using the KECA for dimensionality reduction.

4. VELM Parameters Selection

As a typical type of SLFN, the number of hidden layer nodes, L, is of significance for the performance of the ELM classifier. To determine the optimum node number, a single ELM with different hidden layer nodes was trained and tested based on the experimental data from ASHRAE RP-1043 without dimensionality reduction. The test results are shown in Fig. 7. As seen, since the learning parameters of hidden layer nodes were randomly generated, the fault diagnosis accuracy fluctuated under different hidden layer nodes. Whereas the fault diagnosis performance could be remarkably improved as increasing the hidden nodes to about 80. The highest fault diagnosis accuracy could be achieved at 83.7% for a single ELM with 77 hidden layer nodes. Therefore, the number of hidden nodes for the three individual ELMs was fixed at 77 in the current study.

After obtaining the optimum number of hidden layer node for a single ELM, the number of individual ELM should be further determined. Therefore, VELM based classifiers with different number of ELM (i.e., 1, 3, 5, 7, 9) were trained and tested. Considering the randomness of the initial learning parameters, 50 trials for each VELM were carried out so that the average and maximum fault accuracy based on different VELMs could be evaluated. The results are shown in Fig. 8. As seen, the average and maximum fault diagnosis accuracy for 50 trials could be improved when the number of ELM was increased 1 to 3. However, when further increasing the ELM number, the fault diagnosis performance was degraded due to the problem of overfitting. Therefore, in the current study, three ELMs were adopted in the proposed fault diagnostic model.

5. Fault Identification Results

After determining the key parameters of the proposed KECA-VELM scheme, the fault diagnostic model could be trained and further tested using the experimental data from ASHRAE RP-1043. There were totally 640 experimental samples which were separated into two parts: 480 samples (75% of the total samples) were randomly selected for training the fault diagnostic model, while the remaining 160 samples (25% of the total samples) were then used for testing. For the training dataset, 480 samples contained eight categories, i.e., seven typical faults together with the normal operation, with each including 60 samples. The testing dataset of 160

samples also included eight categories with each containing 20 samples.

To illustrate the effectiveness of the proposed fault diagnosis method, another three commonly used classifiers, i.e., BP neural network (BPNN), single ELM and VELM, were also implemented and their corresponding fault identification results were compared to that by KECA-VELM. In the BPNN, 121 hidden layer nodes were selected through trial and error, and the activation functions for the hidden layer and output layer were hyperbolic tangent function and sigmoid function, respectively. For the ELM classifier, an SLFN with the same number of hidden layer nodes used in the KECA-VELM, namely, 77 hidden nodes, was adopted, but no data decomposition was implemented. In terms of the VELM based method, same as the proposed method, three individual ELMs were utilized but the input data were not transformed to a low-dimensional feature space.

Based on the four established fault diagnostic models, their fault diagnosis results could be acquired and are shown in Fig. 9. In addition, for better illustrating the fault diagnosis performance under these four methods, Fig. 8 gives the results of their corresponding confusion matrixes. It should be pointed out that normal operation was treated as a special kind of fault in the current research; thus the fault detection together with fault diagnosis could be considered as a multi-classification problem. Therefore, the proposed algorithm could be adopted for fault detection. A closer look at the fault diagnosis results for normal operation (fault code 0), showed that a lower false alarm rate could be achieved using the proposed KECA-VELM method. For the BPNN, 7 out of 20 normal samples were misrecognized as anomalies with a reported false alarm rate of 35%. In terms of the ELM and VELM based methods, as shown in Fig. 9(b) and (c), 5 out of 20 and 6 out of 20 normal samples were incorrectly identified as anomalies. When using the KECA-VELM method, only one normal sample was falsely identified and the false alarm rate was remarkably reduced to 5%, demonstrating the effectiveness of the proposed method for chiller fault detection.

It was previously shown that among the seven typical chiller faults, the faults of ReduCF, RefOver and ExcsOil were relatively harder to identify as compared to the other four faults, particularly at their incipient stages [23]. Therefore, taking ExcsOil (fault code 7) as an example, 40% of the testing samples were correctly identified based on the BPNN based classifier, while 10%, 15%, 30% and

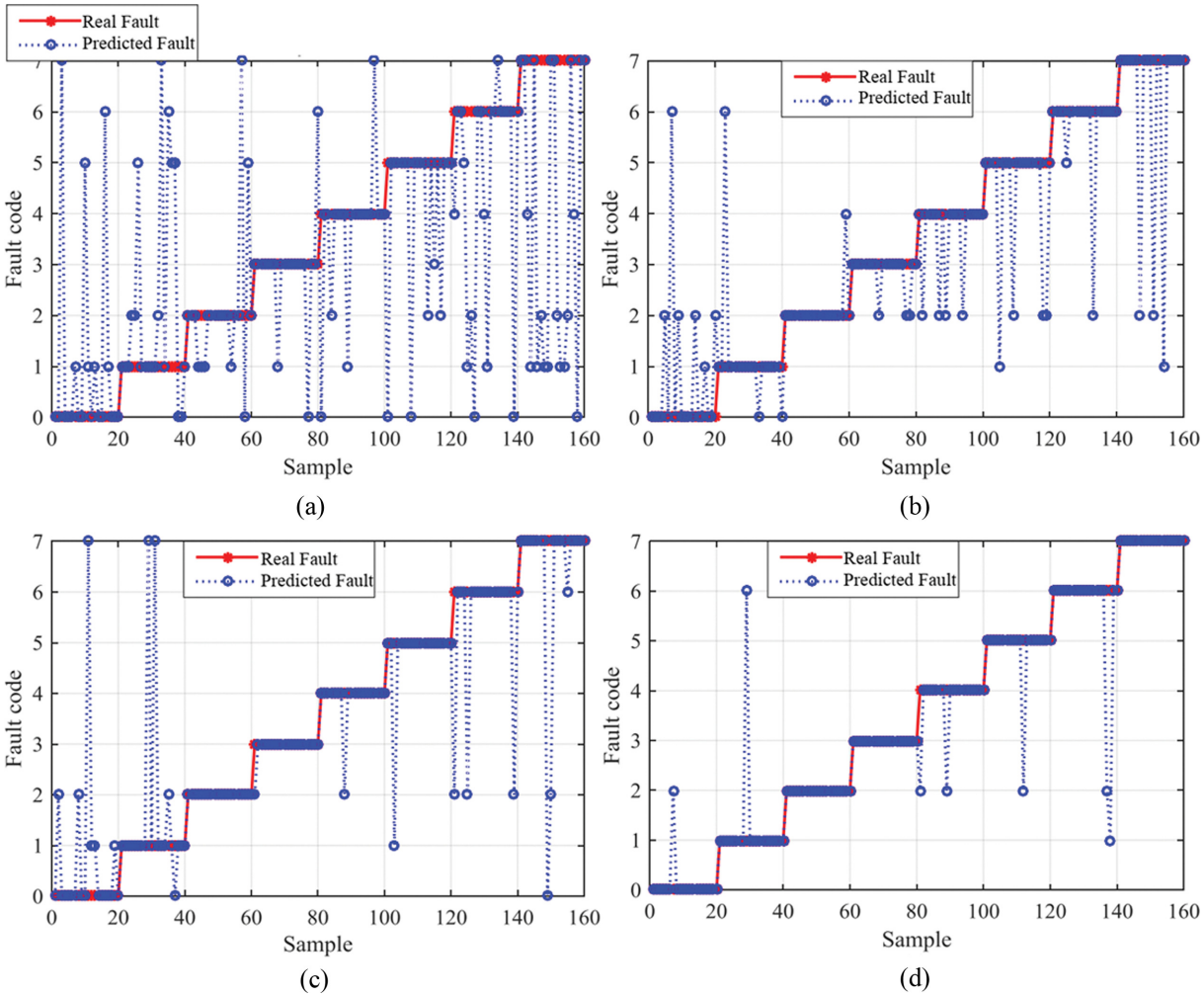

Fig. 9. Fault diagnosis results under different classification methods: (a) BPNN; (b) ELM; (c) VELM; (d) KECA-VELM.

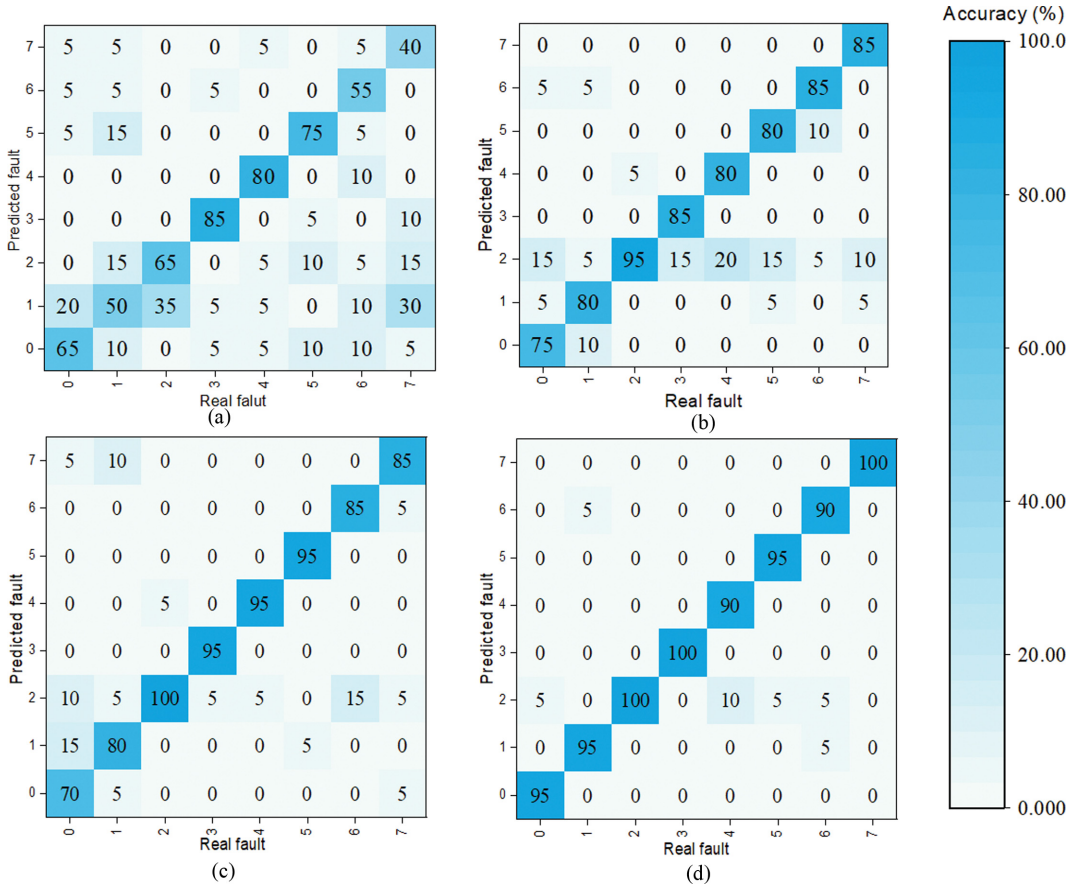

Fig. 10. Confusion matrixes for the fault diagnosis results: (a) BPNN; (b) ELM; (c) VELM; (d) KECA-VELM.

5% were misclassified as ConFoul (fault code 3), ReduEF (fault code 2), ReduCF (fault code 1) and Normal (fault code 0), respectively. When using the ELM and VELM methods, both of their fault diagnosis accuracies for ExcsOil could be significantly improved to 85%. The best classification performance with a reported fault diagnosis accuracy of 100% for ExcsOil was achieved when using the proposed KECA-VELM based fault diagnosis method. 250% improvement of fault diagnosis accuracy was realized in comparison to that of conventional BPNN. With respect to the fault of RefOver (fault code 6), 90% testing samples could be successfully identified using the KECA-VELM classifier larger than that in the case of using the other three classifiers. Moreover, the proposed KECA-VELM classifier was more sensitive to the faults of ReduEF (fault code 2), ConFoul (fault code 3) and ExcsOil (fault code 7), and all their corresponding fault samples could be correctly diagnosed.

Fig. 10 shows the fault diagnosis results as expressed in terms of the confusion matrixes. As seen, the fault diagnosis accuracy of KECA-VELM for all the typical faults except NonCon (fault code 4) could be significantly improved as compared to the other three methods. The degradation of fault diagnosis performance for NonCon may be because the relevant information that was sensitive to this fault may have been lost when performing the KECA based data decomposition. Although 90% of NonCon samples could be successfully identified using the KECA-VELM classifier, smaller than that in the case of using VELM classifier, it was acceptable for practical applications. In summary, the overall average fault diagnosis accuracy for the four classifiers was 64.3% (BPNN), 83.8% (ELM), 88.1% (VELM) and 95.6% (KECA-VELM), respectively. The KECA-VELM based chiller fault diagnosis method outperformed the other three methods by about 48.7%, 14.1% and 8.5%, respectively. The best classification performance as expressed in terms of the highest fault diagnosis accuracy could be achieved using the proposed fault diagnosis method. Therefore the KECA aided VELM based method can be adopted as a powerful classifier for realizing the fault detection and diagnosis of water chillers.

DISCUSSION

The improvement of fault diagnosis performance for the proposed KECA-VELM method is due to the following aspects. In comparison to the conventional BPNN based classifier using the gradient-descent based learning algorithm, the learning parameters of hidden nodes for ELM are randomly assigned and independent of training samples. As a tuning free algorithm, the risk of local minima and over-fitting, which may suffer in the traditional BPNN, can be significantly reduced when using the ELM algorithm for multi-class classification. Consequently, a better generalization performance can be obtained. Furthermore, instead of a single ELM, through performing multiple independent ELM training and integrating with the majority voting method, the problem of misclassi-

fication for the samples near the nonlinear classification boundary could be addressed. Hence, VELM based classifier outperformed the traditional ELM. Moreover, by carrying out the KECA based data decomposition before performing classification, the computation cost could be minimized and at the same time most redundant information could be filtered out. Therefore, with the aid of KECA decomposition technique, a better fault diagnosis performance could be acquired.

On the other hand, the fault diagnosis results aforementioned were obtained using the experimental data from ASHRAE RP-1043 without feature selection. As a matter of fact, proper feature selection can improve FDD performance, while a poor one may negatively influence its performance. In chiller FDD, 16 out of 64 variables were generally selected for further dimensionality reduction [14]. However, the features selected may be different with the variation of FDD method. For example, instead of 16, eight variables were selected when performing SVDD based method for fault detection [15]. Wang et al. [16] selected nine variables as input features, while Huang et al. [23] used ten variables for associative classifier based fault diagnostic model development. In this regard, more efforts will be made to examine the proposed method with feature selection in the near future. It is our belief that the fault diagnosis performance could be improved with the integration of KECA and VELM after performing an appropriate feature selection.

CONCLUSIONS

This paper reports the development of an effective fault diagnosis method for water chillers with the integration of KECA and VELM. A KECA based data decomposition scheme which tried to preserve the maximum Rényi entropy of the original data was performed to reduce the model complexity and computational cost. VELM classifier with three independent ELM and 77 hidden nodes in each ELM was then developed for fault identification.

The experimental data of seven typical faults together with the normal operation from ASHRAE RP 1043 were employed to train and test the proposed KECA-VELM fault diagnosis method. In comparison to another three fault diagnosis methods, i.e. BPNN, ELM and VELM, the best performance could be achieved using the proposed method. Main conclusions are summarized as follows:

1. In terms of the normal operation, the reported false alarm rate based on KECA-VELM method was only 5% smaller than that on BPNN (30%), ELM (20%) and VELM (30%) methods.

2. The KECA-VELM was quite sensitive to the faults of ReduEF, ConFoul and ExcsOil, and 100% fault samples could be correctly identified for these three faults. Although the proposed classifier was less sensitive to the faults of NonCon and RefOver, their fault diagnosis accuracy of 90% could be accepted in practical application.

3. The overall average fault diagnosis accuracy for the proposed KECA-VELM classifier was 95.6%, much larger than the BPNN classifier (64.3%), ELM classifier (83.8%) and VELM classifier (88.1%).

In short, it is concluded that the proposed KECA-VELM algorithm can be an effective technique for both fault detection and fault diagnosis. On the other hand, the limitation of the current study is that no feature selection is included in the proposed fault diagnostic model. Therefore, further studies will be carried out to examine the feasibility of the proposed fault diagnosis method with a proper feature selection.

ACKNOWLEDGEMENTS

The financial supports for the Natural Science Foundation of Zhejiang Province (Project No. LQ19E060007 and No. LY20F030010) and The Science and Technology Project of Zhejiang Province (Project No. LGG21F030009) are gratefully acknowledged.

NOMENCLATURE

H_2 : Rényi quadratic entropy [bit]
s_n : geometrically weighted variance
b : threshold of hidden node
Δt : time interval between measurements [s]
$K(\cdot)$: kernel function
$p(\cdot)$: probability density function
$h(\cdot)$: activation function
λ : eigenvalue
σ : kernel width
ψ : element Rényi entropy
τ_{ss} : time window length [s]
x : a sample vector
w : weight vector connecting the hidden nodes and the input nodes
$\boldsymbol{\beta}$: weight vector connecting the hidden nodes and the output nodes
e : eigenvector
K : kernel matrix
I : vector of ones
D : diagonal matrix storing the eigenvalues
E : eigenvector matrix
H : hidden layer output matrix
$\mathbf{H}^{\dagger}$: Moore-Penrose generalized inverse of **H**
O : output matrix
T : target output matrix

Abbreviations

A/C : air conditioning
AHU : air handling unit
ANN : artificial neural network
BPNN : back propagation neural network
CPV : cumulative percent variance [%]
DX : direct expansion
ELM : extreme learning machine
FDD : fault detection and diagnosis
HVAC : heating, ventilation and air conditioning
KECA : kernel entropy component analysis
PC : principal component
PCA : principal component analysis
SL : severity level
SLFN : single hidden layer feedforward neural network
SVM : support vector machine
VELM : voting based extreme learning machine

VRF : variable refrigerant flow

REFERENCES

1. IEA, The Future of Cooling in China, International Energy Agency (2019).
2. IEA, The Future of Cooling, International Energy Agency (2018).
3. M. C. Comstock, *Development of analysis tools for the evaluation of fault detection and diagnostics in chillers*, Purdue University (1999).
4. S. Katipamula and M. R. Brambley, *HVAC&R Research*, **11**(2), 169 (2005).
5. S. Katipamula and M. R. Brambley, *HVAC&R Research*, **11**(1), 3 (2005).
6. Y. Shin, S. W. Karng and S. Y. Kim, *Int. J. Refrig.*, **40**, 152 (2014).
7. L. Sun, J. Wu, H. Jia and X. Liu, *Chin. J. Chem. Eng.*, **25**(12), 1812 (2017).
8. C. Fan, D. Yan, F. Xiao, A. Li, J. An and X. Kang, *Build. Simul.-China*, **14**(1), 3 (2021).
9. H. Han, Z. K. Cao, B. Gu and N. Ren, *HVAC&R Research*, **16**(3), 295 (2010).
10. Y. Guo, Z. Tan, H. Chen, G. Li, J. Wang, R. Huang, J. Liu and T. Ahmad, *Appl. Energy*, **225**, 732 (2018).
11. Y. Guo, G. Li, H. Chen, J. Wang, M. Guo, S. Sun and W. Hu, *Appl. Therm. Eng.*, **125**, 1402 (2017).
12. S. Li and J. Wen, *Energ. Buildings*, **68**, 63 (2014).
13. K.-P. Lee, B.-H. Wu and S.-L. Peng, *Build. Environ.*, **157**, 24 (2019).
14. Y. Zhao, S. W. Wang and F. Xiao, *Appl. Energy*, **112**, 1041 (2013).
15. G. N. Li, Y. P. Hu, H. X. Chen, L. M. Shen, H. R. Li, M. Hu, J. Liu and K. Sun, *Energ. Buildings*, **116**, 104 (2016).
16. Z. W. Wang, L. Wang, K. F. Liang and Y. Y. Tan, *Appl. Therm. Eng.*, **141**, 898 (2018).
17. Z. Du, X. Jin and Y. Yang, *Appl. Energy*, **86**(9), 1624 (2009).
18. Z. Du, B. Fan, X. Jin and J. Chi, *Build. Environ.*, **73**, 1 (2014).
19. C. C. Chang and C. J. Lin, *ACM Trans. Intell. Syst. Technol.*, **2**(3), 1 (2011).
20. J. Liang and R. Du, *Int. J. Refrig.*, **30**(6), 1104 (2007).
21. H. Han, B. Gu, J. Kang and Z. R. Li, *Appl. Therm. Eng.*, **31**(4), 582 (2011).
22. K. Yan, W. Shen, T. Mulumba and A. Afshari, *Energ. Buildings*, **81**, 287 (2014).
23. R. Huang, J. Liu, H. Chen, Z. Li, J. Liu, G. Li, Y. Guo and J. Wang, *Appl. Therm. Eng.*, **136**, 633 (2018).
24. G.-B. Huang, Q.-Y. Zhu and C.-K. Siew, *Neurocomputing*, **70**(1), 489 (2006).
25. G. Huang, H. Zhou, X. Ding and R. Zhang, *IEEE T. Syst. Man Cy. B*, **42**(2), 513 (2012).
26. W. Zong and G.-B. Huang, *Neurocomputing*, **74**(16), 2541 (2011).
27. A. A. Mohammed, R. Minhas, Q. J. Hu and M. A. Sid-Ahmed, *Pattern Recogn.*, **44**(10), 2588 (2011).
28. Y. Xu, Y. Dai, Z. Y. Dong, R. Zhang and K. Meng, *Neural Comput. Appl.*, **22**(3), 501 (2013).
29. M. Zhang, X. Liu and Z. Zhang, *Chin. J. Chem. Eng.*, **24**(8), 1013 (2016).
30. S. Haidong, J. Hongkai, L. Xingqiu and W. Shuaipeng, *Knowl. Based Syst.*, **140**, 1 (2018).
31. Z. Chen, L. Wu, S. Cheng, P. Lin, Y. Wu and W. Lin, *Appl. Energy*, **204**, 912 (2017).
32. J. Cao, Z. Lin, G.-B. Huang and N. Liu, *Inf. Sci.*, **185**(1), 66 (2012).
33. Y. Chen and L. Lan, *Energ. Buildings*, **41**(8), 881 (2009).
34. Z. M. Du, X. Q. Jin and L. Z. Wu, *Build. Environ.*, **42**(9), 3221 (2007).
35. X. Yu, J. Wu and Y. Gao, *CIESC J.*, **71**(7), 3151 (2020).
36. R. Jenssen, *IEEE Trans. Pattern Anal. Mach. Intell.*, **32**(5), 847 (2010).
37. Y. Xia, Q. Ding, Z. Li and A. Jiang, *Build. Simul.- China*, **14**(1), 53 (2021).
38. L. Bai, Z. Han, J. Ren and X. Qin, *Appl. Soft Comput.*, **92**, 106245 (2020).
39. A. Rényi, *On measures of entropy and information*, In Proceedings of the Fourth Berkeley Symposium on Mathematical Statistics and Probability, Volume 1: Contributions to the Theory of Statistics. The Regents of the University of California (1961).
40. E. Parzen, *Ann. Math. Statis*, **33**(3), 1065 (1962).
41. R. Jenssen, T. Eltoft, M. Girolami and D. Erdogmus, *Kernel maximum entropy data transformation and an enhanced spectral clustering algorithm*, in Conference on Advances in Neural Information Processing Systems (2006).
42. D. Serre, *Matrices: Theory and applications*, Second edition, New York, Springer (2010).